J. exp. Biol. ***192****, 129–145 (1994)*
Printed in Great Britain © The Company of Biologists Limited 1994

UNDULATORY SWIMMING: HOW TRAVELING WAVES ARE PRODUCED AND MODULATED IN SUNFISH (*LEPOMIS GIBBOSUS*)

JOHN H. LONG, JR, MATTHEW J. MCHENRY AND NICHOLAS C. BOETTICHER
Department of Biology, Vassar College, Poughkeepsie, New York 12601, USA

Accepted 17 March 1994

Summary

We have developed an experimental procedure in which the *in situ* locomotor muscles of dead fishes can be electrically stimulated to generate swimming motions. This procedure gives the experimenter control of muscle activation and the mechanical properties of the body. Using pumpkinseed sunfish, *Lepomis gibbosus*, we investigated the mechanics of undulatory swimming by comparing the swimming kinematics of live sunfish with the kinematics of dead sunfish made to swim using electrical stimulation. In electrically stimulated sunfish, undulatory waves can be produced by alternating left–right contractions of either all the axial muscle or just the precaudal axial muscle. As judged by changes in swimming speed, most of the locomotor power is generated precaudally and transmitted to the caudal fin by way of the skin and axial skeleton. The form of the traveling undulatory wave – as measured by tail-beat amplitude, propulsive wavelength and maximal caudal curvature – can be modulated by experimental control of the body's passive stiffness, which is a property of the skin, connective tissue and axial skeleton.

Introduction

Fishes swim by generating undulatory waves – bends of the body that propagate from head to tail and produce thrust. Although the thrust generation of undulatory waves has been investigated from an external, hydrodynamic perspective, less attention has been devoted to the internal mechanisms driving this motion. Our goal is to determine how active muscle interacts with the passive median fins, skin, muscular septa and axial skeleton to produce steady undulatory motion. To this end, we performed experiments with whole fish to test the predictions of several models of undulatory swimming.

Three undulatory models focus on the function of red muscle. In the latest, red muscle appears to power the undulatory motion of scup, *Stenotomus chrysops*, by contracting in phase with local body bending (Rome *et al.* 1993). Red muscle acting in this manner produces positive power – as measured by the mechanical work of isolated muscle bundles subjected to physiological strains and activation – all along the body, but primarily in the caudal region. In contrast, red muscle in the caudal section of carp,

Key words: axial muscle, stiffness, locomotor power, axial skeleton, skin, *Lepomis gibbosus.*

Cyprinus carpio, is thought to produce net negative power, as estimated using *in vivo* electromyography (EMG) activity patterns (Van Leeuwen *et al.* 1990). Negative power is also thought to be produced in the caudal muscles of lamprey, *Ichthyomyzon unicuspis* (Williams *et al.* 1989; Curtin and Williams, 1990). Negative power in the caudal muscles would resist bending by stiffening the body, while the precaudal muscles would produce the positive power for swimming. Regional differences in muscular function were predicted from a third model, one in which kinematics of steadily swimming saithe, *Pollachius virens*, were used to estimate red muscle force balancing hydrodynamic forces (Hess and Videler, 1984). The model predicted that the red muscles on one side of the body (ipsilateral) contract simultaneously, generating bending moments in a standing wave, which, in turn, generates the traveling wave of undulation.

These red muscle models are appropriate for the slow and intermediate speeds at which only red muscle operates; at faster speeds, white muscle becomes active in addition (Rome *et al.* 1992). Furthermore, the three models examine muscle function independently of the body's passive mechanical properties and structures. Mechanical properties and locomotor structures are integrated with muscle in two qualitative models. Blight (1976, 1977) postulated that the body's mechanical properties control undulatory motion. Using EMG, he measured electrical activity of the precaudal myomeres in the embryos of the palmate newt *Triturus helveticus*, while the caudal myomeres remained electrically inactive (Blight, 1976). From these data, he proposed that traveling waves of EMG activity were not required for undulatory motion – instead, the undulatory motion generated anteriorly could passively propagate in a manner dependent upon the mechanical properties of the body. When internal forces, both active and passive, restrict bending during lateral movement, that part of the body is said to be 'stiffness dominated'. When external forces, from resistance of the water, cause or restrict bending during lateral movement, that part of the body is said to be 'resistance dominated'. Complementary to Blight's mechanical properties model is the structural model of Wainwright (1983). He proposed that skin, axial skeleton and horizontal septa were, by their connections to muscle, important in transmitting forces from muscle to propulsive elements. This model assumes that since the bulk of the lateral muscle, red and white combined, is located precaudally, it produces the most locomotor force, which is then transmitted to the caudal fin.

Clearly, the primary mechanisms of undulatory swimming differ in these models. To examine these mechanisms in more detail, we tested the following sets of predictions. (1) *Power generation* (generalized to include both red and white muscle): undulatory swimming is powered primarily by either the caudal musculature (Rome *et al.* 1993) or the precaudal musculature (Van Leeuwen *et al.* 1990). (2) *Wave generation*: undulatory waves are generated either by precaudal muscle alone (Blight 1976, 1977) or by simultaneous alternating contractions of the ipsilateral musculature (Hess and Videler, 1984). (We did not test the prediction that sequential contraction generates waves.) (3) *Wave modulation*: undulatory waves can be modulated by the mechanical properties of the body (Blight, 1976, 1977; Van Leeuwen *et al.* 1990). (4) *Power transmission*: axial connective tissues transmit muscular power from the precaudal musculature to the caudal fin (Wainwright, 1983).

To test these predictions, we needed an experimental system in which the experimenter

controls muscle activation, the mechanical properties of the body and the integrity of axial structures. To meet these requirements, we developed electrically stimulated swimming, a procedure in which the investigator controls the 'swimming' of a dead fish through stimulating electrodes implanted in the locomotor muscle. Using pumpkinseed sunfish, *Lepomis gibbosus*, we compared the swimming motions of electrically stimulated fish, both intact and surgically altered, with those of living fish.

Materials and methods

Study species

All *Lepomis gibbosus* were collected by seine or rod and reel during July 1992 and May 1993 from Sunset Lake, Vassar College, Poughkeepsie, New York. Fish were held in tanks at room temperature prior to experiments. For live kinematics, individuals were transferred directly from the holding tank to the flow tank, which contained water within 1 ˚C of the holding tank temperature (18–20 ˚C). For electrically stimulated swimming experiments, individuals were killed with a 1:5000 overdose of MS-222 (Argent Chemical Laboratories).

Electrically stimulated swimming

Following death, fish were implanted with stimulating electrodes in the left and right precaudal musculature (Fig. 1). Electrodes were made of 0.2 mm insulated solid-core wrapping wire with 15 mm of insulation removed at the tip. Electrodes were implanted using a 20 gauge hypodermic needle inserted into the superficial muscle of the first four myomeres, parallel to the skin, with the exposed tip flared and oriented in the direction opposite to insertion to prevent slippage. A negative electrode was placed below and a positive electrode above the horizontal septum.

Two stimulators (Phipps and Bird model 611) provided each side of the fish with the voltage for muscle activation. Voltages were 20 V d.c., which elicited maximum swimming speed prior to muscle fatigue. Only trials prior to muscle fatigue were analyzed. The stimulators were triggered to activate the left and right lateral musculature alternately, at a frequency of 3 Hz with square-wave pulses. The duration of the stimulus was 30 ms or about 9 % of the tail-beat cycle, which corresponds to the time that ipsilateral muscles are simultaneously active in carp (Van Leeuwen *et al.* 1990).

Stimulation of precaudal myomeres on one side simultaneously activated all ipsilateral musculature. This was determined using a high-speed video system and muscle pressure measurements in the following manner. Stimulating electrodes were implanted in a dead sunfish as described above for electrically stimulated swimming. In addition, stimulating electrodes were implanted in the caudal musculature. Between first the precaudal and then the caudal electrodes, a pressure transducer (Gould model P23D) attached to a strain gauge amplifier (Omega model DMD-520) was connected intramuscularly *via* a hypodermic needle filled with vegetable oil. Pressure was used as a direct measurement of muscle force; it has been used successfully for this purpose in human skeletal muscle (Sejersted *et al.* 1984; Ballard *et al.* 1992). Using a high-speed video system (NAC model HSV-500) at 500 frames s^{-1}, we videotaped the fish's response to stimulation in a still-

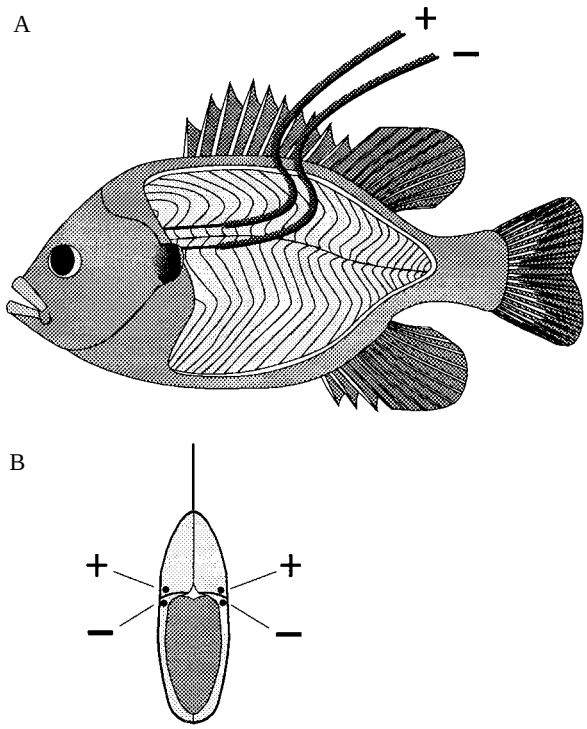

Fig. 1. Position of implanted electrodes for electrically stimulated swimming. (A) Lateral view of a dead pumpkinseed sunfish, showing the axial position of stimulating electrodes in the myomeres. Bare electrode tips (black) were located in the first four myomeres, with the positive electrode above and the negative electrode below the horizontal septum. The skin has been removed in this diagram only to show the positions of the myomeres and horizontal septum. (B) Transverse view through the precaudal body at the level of the electrodes, showing the depth and placement of electrodes relative to the horizontal septum. All red and white muscle on one side was simultaneously stimulated (see Materials and methods).

water tank. Both the stimuli and the pressure were recorded on screen. A delay of 10–12 ms from stimulation to muscle pressure was measured in both precaudal and caudal regions with either precaudal or caudal stimulation, demonstrating simultaneous ipsilateral contraction with local stimulation. The changes in pressure, from 8 to 16 kPa, were not the result of body bending, since these pressures appeared before any movement was detected.

Kinematic analysis

For electrically stimulated swimming, each dead sunfish with implanted electrodes was suspended by its electrode wires from a platform floating on a ‘frictionless’ air track into a still-water tank (Fig. 2). The frictionless air track reduced forces associated with wire movement as the fish swam across the tank; since we analyzed only constant-velocity swimming segments, any inertia caused by the initial acceleration of the platform was eliminated. A mirror at 45 ° placed under the tank allowed imaging of the ventral surface

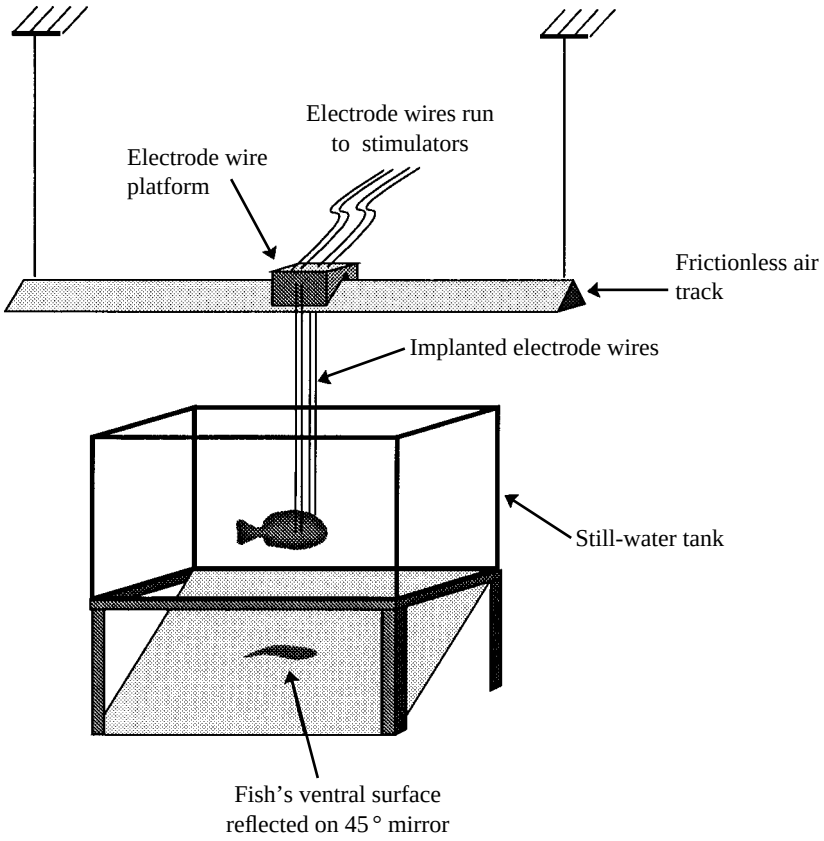

Fig. 2. Experimental set-up for electrically stimulated swimming. A dead fish was attached *via* stimulating electrodes to a 'frictionless' air track. The electrodes led to electrical stimulators that delivered alternating square-wave impulses to the left and right sides of the musculature. The fish swam from left to right and its ventral surface was videotaped through a 45° mirror.

of the fish without refraction of the image due to waves at the surface of the tank. Fish were videotaped (Panasonic model AG-450 SVHS camcorder) at 30 frames s^{-1} with an exposure time of 1 ms.

Live sunfish were videotaped at constant velocities in a flow tank (Vogel, 1981). Two flow straighteners reduced turbulence; the first was angled at 75° relative to the bottom of the tank in order to flatten the parabolic vertical velocity gradient. The second straightener was oriented at 90° relative to the bottom of the tank. The flattened velocity gradient allowed fish to swim between 5 and 15 cm off the flow tank's floor and to be in flow velocities within 10 % of the mean velocity in that 10 cm section of the water column. A mirror was placed at 45° under the working section, which was built with a transparent bottom, so that ventral images of the fish could be used.

For live sunfish, eight swimming speeds (in body lengths s^{-1}) were chosen: 1.4, 1.7, 2.1, 2.4, 2.7, 3.1, 3.5 and 4.0. The slowest speed was the first at which some individuals

swam using axial undulation without pectoral fin rowing. The highest speed was the last at which some individuals could sustain a constant velocity. Fork length, the axial distance from the anteriormost tip of the rostrum to the apex of the angle produced by the two caudal lobes, was used as body length. For analysis, the only sequences used were those in which the fish (1) did not use pectoral fins, (2) did not move forwards or backwards in the flow for three tail-beats, and (3) stayed within the calibrated flow space (lateral views were videotaped to ensure compliance).

Data points on the video frames were digitized using a computer (Commodore Amiga 1000) and a freeze-frame video deck (Sony SVO-9200-MDR SVHS). Each time-coded frame was overlaid on the computer screen. Using a cursor within a Basic program (Crenshaw, 1992), 15 points along the ventral midline of the fish, starting at the rostrum and ending at the tip of the caudal fin, were digitized. The following kinematic variables were calculated for an individual at a given speed: (1) tail-beat frequency, (2) tail-beat amplitude, (3) rostral amplitude, (3) anterior propulsive wavelength, (4) posterior propulsive wavelength, and (5) maximal caudal curvature. Tail-beat frequency (Hz) was the inverse of the average time of three tail-beat cycles. Tail-beat amplitude (cm) was the average peak-to-trough displacement of three tail-beats. Rostral amplitude (cm) was the average peak-to-trough displacement of three cycles of the rostrum. Anterior and posterior propulsive wavelengths (% body length) were the half-wave components of the propulsive wave, a standard kinematic variable that is the apparent wavelength of the body when midline images are superimposed about the axis of progression (Webb and Keyes, 1982; Webb, 1986, 1988). Maximal caudal curvature was the maximum non-dimensionalized curvature in the caudal section of the body. To find maximal caudal curvature, the 15 midline points at the time of maximal body bending – when the propulsive wavelength was smallest – were fitted by a least-squares third-, fourth- or fifth-order polynomial equation (CricketGraph, version 1.3). The resulting equation needed an r^2 value of 0.99 or higher to be judged a close fit. To achieve a close fit, some midlines were divided into two sections and fitted separately. Curvature, κ (in units of m^{-1}, the inverse of radius of curvature) at any point, x, was determined using the following equation (Gillet, 1984):

$$\kappa = \frac{|y''|}{[1 + (y')^2]^{1.5}}, \tag{1}$$

where y is the polynomial equation for the midline, y' is its first derivative and y'' is its second derivative. The accuracy of curvature determined in this way is 95±2.1 % (± 1 S.D.) (Long, 1994). To non-dimensionalize curvature, the relative curvature was calculated as the product of curvature (m^{-1}) and fork length (m) of the individual fish.

Experimental design

We designed our experiments so that the data could be analyzed using a fully factorial multiple analysis of variance (MANOVA). For response (dependent) variables, we used swimming speed and four variables that are constant in living sunfish with respect to swimming speed: tail-beat amplitude, anterior propulsive wavelength, posterior propulsive wavelength and maximal caudal curvature. Tail-beat frequency was held

constant at 3 Hz in our experimental treatments. Rostral amplitude was not used because, in living sunfish, it increases linearly with increasing swimming speed (see Results), which, in turn, varies with experimental treatment.

The independent variable in our design was experimental treatment, which had five categories with three different individuals in each category for a sample size of 15: (1) live, (2) whole-with-fins, (3) whole-without-fins, (4) severed and (5) ablated. For the live category, live sunfish were swum in the flow tank at a speed of 2.1 lengths s^{-1}. This was the slowest speed at which at least three pumpkinseeds swam without using their pectoral fins. Categories 2–5 were electrically stimulated swimming procedures performed on dead fish. For the whole-with-fins category, dead fish were made to swim electrically with their median fins in place and erect; paired fins were removed. For the whole-without-fins category, the dorsal and anal fins were removed, leaving only the caudal fin intact. For the severed treatment, dead fish were swum electrically with only their caudal fin intact and with the caudal musculature, held in place by the skin, rendered non-functional by severing the horizontal septa, spinal nerves and myotomes. For the ablated treatment, the median fins, caudal musculature and skin were removed, leaving only the axial skeleton connecting the precaudal body to the caudal fin. The ablated treatment lowers the mass of the body by approximately 10 % and the mass of the caudal region by 50 %.

The whole-with-fins category tests the prediction that fish with simultaneous ipsilateral contraction can generate an undulatory wave. The severed category tests the prediction that the precaudal muscles alone are sufficient to generate an undulatory wave and to power swimming *via* connective tissues; this indirectly tests whether the caudal muscles could be the primary producers of power. The ablated category tests the prediction that the axial skeleton can transmit locomotor power to the caudal fin. In addition, we planned four comparisons between the treatment categories: (1) live compared with whole-with-fins, to determine whether there are kinematic differences between live and electrically stimulated swimming; (2) whole-with-fins compared with whole-without-fins, to determine whether the anal and dorsal fins affect undulatory kinematics; (3) whole-without-fins compared with severed, to test the prediction that mechanical properties, specifically lower stiffness (see next section), as dictated by the connective tissues, affect undulatory kinematics; (4) severed compared with ablated, to determine whether lower stiffness of the body (see next section), as determined by skin and muscle mass, and lower mass of the caudal region affect undulatory kinematics.

Stiffness tests

To determine body stiffness in each experimental treatment, dead fish were bent laterally using a bending machine (Long, 1992), which was modified to load a section of the fish's body with a quasi-static bending moment (N m) and to measure the resulting angular displacement (rad). The bending moment was measured using a strain gauge attached to one of the grips holding the fish stationary. The other grip holding the fish was attached to a lever arm that pivoted midway between the two grips. The shaft of this pivot was connected to a rotary variable differential transducer (RVDT, Schaevitz model R30D), which measured the angular displacement of the shaft. The free end of the shaft

was activated manually at cycle frequencies below 1 Hz. Voltage signals from the strain gauge and the RVDT were digitally sampled at 20 Hz (Vernier Inc., Universal Laboratory Interface and DataLogger software). The initial linear slope of the plot of bending moment *versus* angular displacement was used as the angular stiffness per unit length of section bent ($k \times l^{-1}$). Angular stiffness k (N m rad^{-1}), which is independent of the section length l, was calculated as the product of the section length and the length-specific stiffness.

The precaudal section of the whole dead fish was bent first, with one grip holding the posterior margin of the neurocranium and the other holding the pectoral girdle [the distance between grips was 12.5±0.76 % (± 1 S.D., N=3) of the fork length]. The caudal section of the whole fish was bent next, with one grip in register with the anterior margin of the anal fin and the other grip in register with the posterior margin of the anal fin [the distance between grips was 6.5±0.17 % (± 1 S.D., N=3) of the fork length]. Bending tests were then repeated after structurally altering the fish in a manner identical to the severed and ablated treatments for electrically stimulated swimming (see above). Three dead fish were bent in this manner prior to *rigor mortis*.

Because repeated measurements were made on the same individuals, a profile analysis of variance, instead of a traditional ANOVA, was used to avoid inflating degrees of freedom through pseudoreplication (Simms and Burdick, 1988). The independent variable was experimental treatment with three categories: whole, severed and ablated. The response variable was angular stiffness, k. Two comparisons were planned. (1) Does stiffness differ between whole and severed treatments? (2) Does stiffness differ between severed and ablated treatments? All statistical tests were conducted using Systat (Wilkinson, 1989).

Results

Live kinematics

In live, steadily swimming pumpkinseed sunfish, we detected a significant linear relationship between swimming speed and two response variables, tail-beat frequency and rostral amplitude (Fig. 3A,B), using regression analysis. In a manner similar to that in other teleosts, tail-beat frequency can be described as a function of swimming speed using the following regression equation y=1.360+1.040x (r^2=0.810, P=0.002), where x is the swimming speed and y is the tail-beat frequency. Rostral amplitude can be described as a function of swimming speed using the regression equation y=−0.014+0.207x (r^2=0.662, P=0.014), where x is the swimming speed and y is the rostral amplitude. For the other four response variables (tail-beat amplitude, anterior propulsive wavelength, posterior propulsive wavelength and maximal caudal curvature), we could not detect a significant non-zero linear slope. This was expected for the tail-beat amplitude and the wavelengths, since they remain constant above slow speeds in some teleosts (Webb, 1988; Webb and Keyes, 1982). The mean tail-beat amplitude was 2.25±0.210 cm (±S.E.M., N=21) (Fig. 3B). The mean anterior propulsive wavelength was 0.55±0.055 % body length (±S.E.M., N=21) (Fig. 3C). The mean posterior propulsive wavelength was 0.46±0.040 % body length (±S.E.M., N=21) (Fig. 3C). The mean maximal

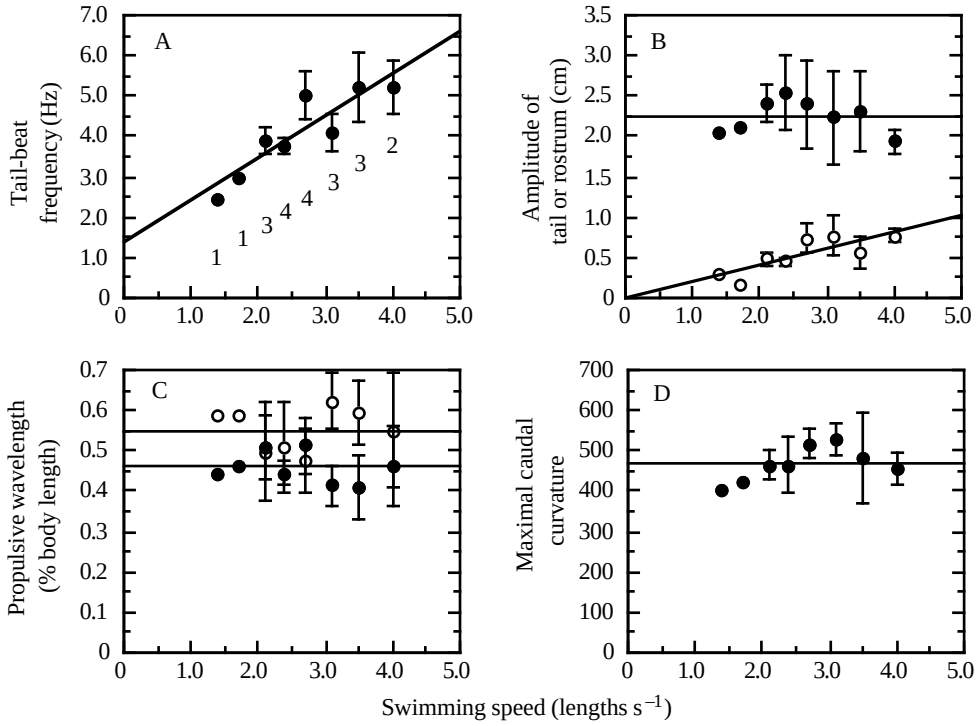

Fig. 3. Kinematics of live, steadily swimming pumpkinseed sunfish. The data points represent the mean value of the kinematic variable for up to four individuals with respect to swimming speed (body lengths s^{-1}). Error bars are 1 S.E.M. (A) Tail-beat frequency. Tail-beat frequency increases linearly with increasing swimming speed. See Results for regression equation. The numbers under each point indicate the sample size at each speed for all kinematic variables. (B) Tail-beat (filled circles) and rostral amplitude (open circles). Tail-beat amplitude is independent of swimming speed. Its average value over the range of speeds is 2.25±0.210 cm (S.E.M., *N*=21). Rostral amplitude increases linearly with increasing swimming speed. See Results for the regression equation. (C) Propulsive wavelength. Anterior (open circles) and posterior (filled circles) half-waves are shown, both of which are independent of swimming speed. For the anterior half-wave, the average value is 0.55±0.055 % body length (S.E.M., *N*=21). For the posterior half-wave, the average value is 0.46±0.040 % body length (S.E.M., *N*=21). (D) Maximal caudal curvature. This non-dimensionalized measure is independent of swimming speed, with an average value of 467±43.1 (S.E.M., *N*=21).

caudal curvature was 467±43.1 (±S.E.M., *N*=21) (Fig. 3D). Note that the number of individuals that swam without using pectoral fins varied with speed (Fig. 3A).

Electrically stimulated swimming

All electrically stimulated sunfish swam using traveling undulations of the body (Fig. 4). For the whole-with-fins treatment category, this supports the prediction that simultaneous ipsilateral contractions of the musculature can generate undulatory waves. Severed, electrically stimulated fish, with caudal muscle deactivated, also swam using undulatory waves, supporting the prediction that precaudal muscles alone are sufficient to

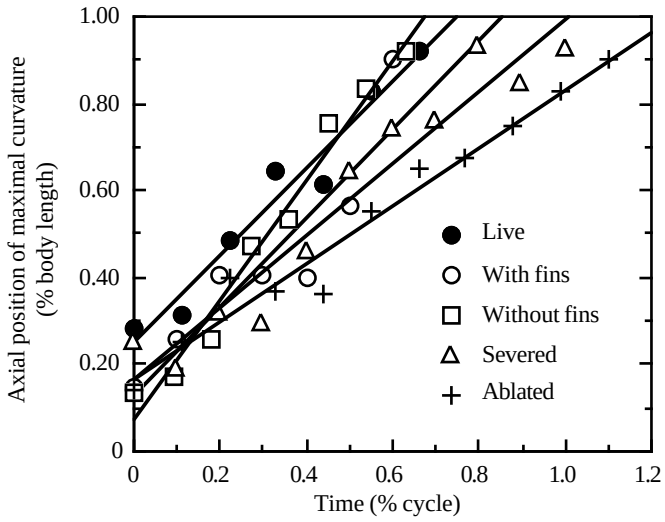

Fig. 4. Undulatory waves in electrically stimulated sunfish travel from head to tail. Movement of the undulatory wave is plotted against time as the axial position of the point of maximal curvature of the midline. Time is given as the percentage of the tail-beat cycle. The data plotted are typical for all treatment categories, which all show traveling waves, as indicated by the rostral–caudal movement of the maximal curvature. Note that in the severed and ablated treatment categories, where body stiffness has been lowered, the waves travel more slowly than in live, with-fins and without-fins treatment categories.

generate and power undulatory swimming. Ablated, electrically stimulated fish also swam using undulatory waves, supporting the prediction that the axial skeleton can transmit sufficient amounts of muscle power to the caudal fin to propel the fish.

The MANOVA detected significant overall differences in four of the five kinematic variables with changes in experimental treatment: swimming speed, tail-beat amplitude, posterior propulsive wavelength and maximal caudal curvature (Fig. 5). Anterior propulsive wavelength did not change significantly with changes in experimental treatment. Mean values (± S.E.M., N=3) for anterior propulsive wavelength in each treatment category were 0.50±0.121 % body length (live), 0.55±0.096 % body length (whole-with-fins), 0.55±0.150 % body length (whole-without-fins), 0.42±0.072 % body length (severed) and 0.44±0.055 % body length (ablated).

Four *post-hoc* comparisons revealed the following significant differences between treatment categories. (1) In the comparison between live and whole-with-fins treatment categories, we detected a significant decrease in the swimming speed (Fig. 5A) and in the posterior propulsive wavelength (Fig. 5C). Swimming speed dropped by 43 %, from a mean of 2.1 to 1.2 lengths s^{-1} (P=0.001). Posterior propulsive wavelength dropped by 35 %, from a mean of 0.51 to 0.33 % body length (P=0.002). These changes correspond to the change from presumed sequential muscle activation in live sunfish to simultaneous ipsilateral activation in electrically stimulated fish. Otherwise, electrically stimulated swimming mimics live swimming in terms of tail-beat amplitude, anterior propulsive wavelength and maximal caudal curvature. (2) In the comparison between whole-with-

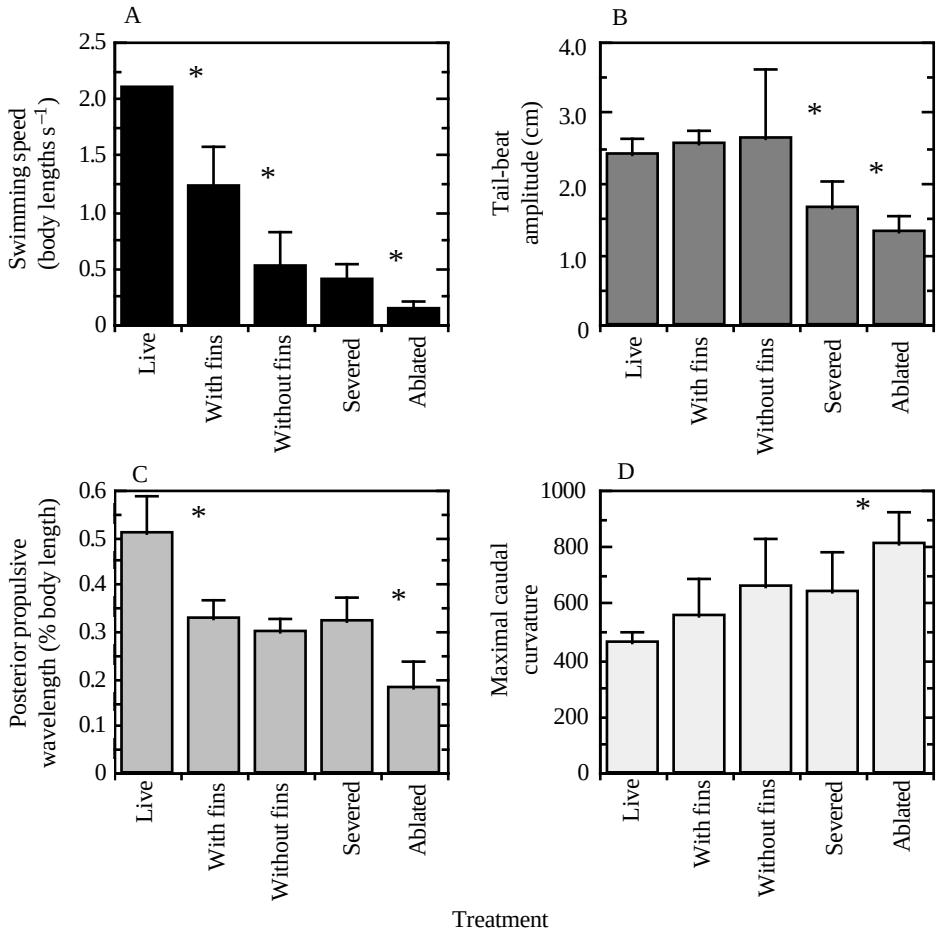

Fig. 5. Swimming kinematics of pumpkinseed sunfish are altered by changes in locomotor morphology. A fully factorial MANOVA (N=15) was conducted with treatment as the independent variable and swimming speed (A), tail-beat amplitude (B), posterior propulsive wavelength (C) and maximal caudal curvature (D) as the dependent variables that varied significantly with experimental treatment. For each dependent variable, four comparisons (contrasts) were made, one between each treatment category. Asterisks indicate significant differences between neighboring treatment categories at P<0.05. Bars show S.E.M.

fins and whole-without-fins treatment categories, we detected a significant decrease in swimming speed (Fig. 5A), which dropped by 57 %, from a mean of 1.2 to 0.52 lengths s^{-1} (P=0.003). The only difference between these two categories is that the anal and dorsal fins have been removed in the whole-without-fins category. (3) In the comparison between whole-without-fins and severed treatment categories, we detected a significant decrease in tail-beat amplitude (Fig. 5B), which dropped by 37 %, from a mean of 2.7 to 1.7 cm (P=0.035). This change corresponds to the deactivation of caudal muscle – by severing nerves, horizontal septa and muscles – which also lowered the stiffness of the body (see Fig. 6). The fact that swimming speed did not change

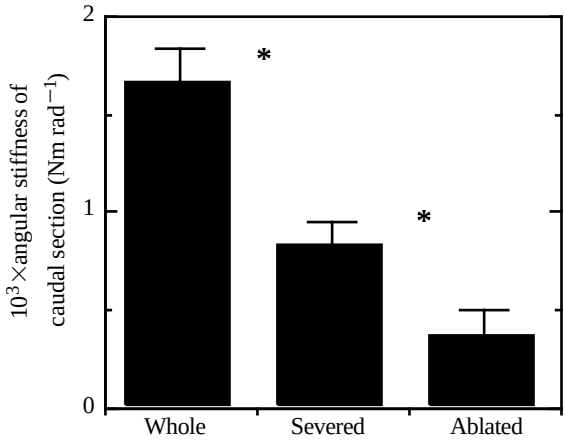

Fig. 6. Stiffness of the body is altered by changes in locomotor morphology. Profile analysis of variance (N=3) was used to analyze the data from the mechanical bending tests, with three experimental treatment categories in the independent variable and angular stiffness as the dependent variable. The two comparisons revealed a significant drop in stiffness with each treatment category. The asterisks indicate a significant difference between the means at P<0.05. Bars show S.E.M.

significantly supports the prediction that most of the muscular power for swimming is generated by the precaudal muscles under these circumstances. (4) In the comparison between severed and ablated treatment categories, we detected a significant decrease in swimming speed, tail-beat amplitude and posterior propulsive wavelength, and a significant increase in maximal caudal curvature (Fig. 5). Swimming speed dropped by 65 %, from a mean of 0.40 to 0.14 lengths s^{-1} (P<0.001). Tail-beat amplitude dropped by 21 %, from a mean of 1.67 to 1.32 cm (P=0.002). Posterior propulsive wavelength dropped by 44 %, from a mean of 0.32 to 0.18 % body length (P=0.001). Maximal caudal curvature increased by 28 %, from a mean of 637 to 815 (P=0.031). These changes in speed and motion correspond to a decrease in body stiffness (Fig. 6) and caudal mass, thus supporting the prediction that stiffness can alter undulatory wave form.

Stiffness tests

The bending stiffness of the caudal region of the pumpkinseed body decreases significantly with the structural changes dictated by experimental treatment (Fig. 6). In the comparison of whole-with-fins with severed categories, we detected a significant drop in angular stiffness (P=0.040), with a decrease of 50 %, from a mean of 1.65×10^{-3} to 0.82×10^{-3} N m rad^{-1}. In the comparison of severed with ablated categories, we detected a significant drop in angular stiffness (P=0.024), with a decrease of 56 %, from a mean of 0.82×10^{-3} to 0.36×10^{-3} N m rad^{-1}. We detected no significant differences in precaudal stiffness with the same structural changes.

Discussion

We have investigated the mechanics of undulatory swimming using the technique of electrically stimulated swimming. By controlling muscle activation, the integrity of

locomotor structures and the stiffness of the body in dead pumpkinseed sunfish, we produced and modulated traveling undulatory waves. These waves were generated by alternating left–right contractions of all the axial muscle. Since this pattern of simultaneous contraction differs from the pattern of sequential contraction seen in live fish, these results should be interpreted with caution.

Powering swimming

Because there is no significant decrease in swimming speed when the caudal muscles are disabled (severed treatment category) in dead sunfish swimming *via* electrical stimulation (Fig. 5A), the precaudal muscle is generating most of the locomotor power in the intact, electrically stimulated fish (without-fins treatment category). Swimming speed is an indicator of power output since it is proportional to the cube root of locomotor power (see Withers, 1992).

This result supports the general prediction, derived from the red muscle model of Van Leeuwen *et al.* (1990), that the anterior muscles in live fish produce most of the locomotor power. However, we found no support for the prediction, derived from the red muscle model of Rome *et al.* (1993), that the posterior muscles produce most of the locomotor power. It is important to note, however, that our experiment does not directly test the model of Rome *et al.* (1993), since it is possible that the simultaneous contraction of all of the muscles altered the phase relationships between posterior muscle contraction and local muscle strain necessary for positive power production caudally.

The pattern of simultaneous contraction in dead, electrically stimulated sunfish (whole-with-fins category) appears to produce less power than the presumed sequential contraction in live sunfish. The speed, and hence power output, of the electrically stimulated sunfish dropped by 43 % compared with live sunfish (Fig. 5A). This decreased power output is correlated with a 35 % drop in the posterior propulsive wavelength (Fig. 5C).

Swimming speed also decreased significantly with the removal of the anal and dorsal fins (Fig. 5A). This result is consistent with the role of these fins in transferring the body's momentum to the surrounding water. As the body accelerates, an 'added mass' of surrounding water, in proportion to the body's volume and the fluid's density, must also be accelerated (Daniel, 1984; Denny, 1988). The force needed to accelerate this added mass, the acceleration reaction, acts in a direction opposite to the motion of the body, thus resisting movement. In the case of fins, their added mass is small because of their low volume, and thus they are highly efficient in transferring energy to the surrounding water (Weihs, 1989). With a lower energy transfer efficiency caused by the removal of fins, more locomotor power would be dissipated in the acceleration reaction, resulting in decreased swimming speed.

Swimming speed, and hence power output, also decreased significantly with the removal of the caudal muscle mass (ablated treatment category, Fig. 5A). Removing this muscle decreases the added mass through volume reduction and decreases bending stiffness through removal of the skin (Fig. 6). Apparently in this case, the decreased acceleration reaction, and its accompanying increase in efficiency, are more than offset

by the drop in stiffness, which decreases the body's ability to transmit power to the caudal fin (see below).

Generating undulatory waves

In a dead sunfish swimming with electrical stimulation, undulatory waves can be generated by alternating left–right contractions of either all the axial muscle (whole-with-fins treatment category, Fig. 4) or just the precaudal muscle (severed treatment category, Fig. 4). These results support the predictions of the models of Hess and Videler (1984) and Blight (1976, 1977) respectively.

At first it is surprising that a simple, alternating contraction of the lateral muscle, which is *not* characteristic of the EMG patterns in live fish (Williams *et al.* 1989; Van Leeuwen *et al.* 1990), produces undulatory motions. From hydrodynamic principles, Hess and Videler (1984) predicted that simultaneous ipsilateral contractions, which would generate a standing wave of bending moment, could in fact create a traveling wave of bending motion. Our results show that Hess and Videler's model is a feasible, if not actual, mechanism for generating undulatory motion. If simultaneous ipsilateral contraction is feasible, why do we not find such patterns in living fish? In fact, we do find this pattern, but in transient rather than steady undulatory swimming. During phase 1 of fast starts in teleosts, the time during which the fish bends from a straight posture into a tight C shape, the ipsilateral musculature is simultaneously activated in bluegill sunfish, *Lepomis macrochirus* (Jayne and Lauder, 1993). In terms of duration of muscle activity, however, the constant activity of electrically stimulated swimming in pumpkinseed sunfish does not resemble the pattern of posteriorly increasing activity in bluegill sunfish (Jayne and Lauder, 1993).

In the severed treatment category, sunfish swim with alternating contractions of only the precaudal muscle. This result supports the prediction that traveling waves can be produced with only the anterior muscles (Blight, 1976, 1977). This prediction is also supported by the observation that EMGs limited to the anterior myomeres are associated with undulations in amphibian tadpoles (Wassersug, 1989) and that undulations can be generated by passive oscillation of anaesthetized *Rana* and *Bufo* tadpoles (Wassersug and von Seckendorff Hoff, 1985).

Modulating undulatory waves

The form of undulatory waves can be altered by the passive control of axial stiffness. Tail-beat amplitude decreased significantly (Fig. 5B) with the removal of skin and muscle (ablated treatment), structural changes that caused a significant decrease in the body's caudal stiffness (Fig. 6). This decrease in stiffness also decreased the posterior propulsive wavelength (Fig. 5C) and increased maximal caudal curvature (Fig. 5D).

The identification of the body stiffness as a determinant of tail-beat amplitude, posterior propulsive wavelength and maximal caudal curvature supports the prediction of Blight's (1976, 1977) hybrid oscillator model. He predicted that mechanical properties of the body, and stiffness in particular, would vary axially and at different swimming speeds, acting either to maintain or to modulate undulatory motion. This result can be understood, in part, in the context of vibratory mechanics. In a single-degree-of-freedom

system, angular stiffness k is the constant of proportionality between an externally applied bending moment M and the resulting angular displacement θ (Den Hartog, 1958):

$$M = k\theta \, . \tag{2}$$

Any bending moment – applied externally *via* hydrodynamic forces or internally *via* muscular forces – will cause a displacement, or bend, inversely proportional to the angular stiffness. The angular displacement, proportional to maximal caudal curvature in our case, will increase as stiffness decreases in a sinusoidally oscillating system driven by a constant-amplitude sinusoidal bending moment. The increased caudal curvature, which reaches its maximum when the tail crosses the midline, decreases tail-beat amplitude and posterior propulsive wavelength.

Transmitting power

Our results support the prediction that the skin and axial skeleton transmit locomotor power from the muscles to the caudal fin (Wainwright, 1983). When the caudal skin and muscle, which had been previously disabled, were removed in the ablated treatment category, the stiffness of the body decreased (Fig. 6), as did the swimming speed (Fig. 5A). Thus, during electrically stimulated swimming, the caudal skin appears to be a transmitter of the locomotor power that is generated by the precaudal muscles. Because the muscles underlying the skin in the severed treatment category were disabled, the skin may not, as predicted for sharks, transmit force generated by radial muscle bulging (Wainwright *et al.* 1978). Instead, the skin may act as a series tendon between the muscle and the caudal fin. Evidence for power transmission *via* the axial skeleton comes from the observation that undulatory swimming is possible with only an axial skeleton connecting precaudal muscle to the caudal fin (Fig. 4). This result supports the long-standing hypothesis that the axial skeleton can function as a power transmitter (Home, 1809; Rockwell *et al.* 1938; Symmons, 1979; Wainwright, 1983; Long, 1992).

Another axial structure implicated as a force and power transmitter is the horizontal septum, which is robust in tuna and mackerel (Westneat *et al.* 1993). Because destruction of the horizontal septum and muscle architecture in sunfish reduced stiffness (Fig. 6), we have evidence that the septum, which connects skin and axial skeleton, stiffens the body passively. However, this structural alteration did not change swimming speed (Fig. 5A), which suggests that the comparatively diffuse horizontal septum of sunfish transmits little or no locomotor power.

The authors wish to thank Bruce Jayne for his advice on the design and calibration of flow tanks. We thank Hugh Crenshaw for the use of his motion analysis software and system and Steve Wainwright for the loan of the Commodore Amiga computer. For constructive comments on this manuscript, we thank Steve Nowicki, Robert Suter, Mark Westneat, Steve Wainwright, Richard Wassersug and two anonymous reviewers. Charles Pell deserves thanks for sharing his insights on undulatory swimming. This work was supported by a grant to J.H.L. from the Office of Naval Research (N00014-93-1-0594). M.J.M. was supported during the summers of 1992 and 1993 by a fellowship from the Undergraduate Research Science Institute, Vassar College.

References

BALLARD, R. E., ARATOW, M., CRENSHAW, A., STYF, J., KAHAN, N., WATENPAUGH, D. E. AND HARGENS, A. R. (1992). Intramuscular pressure measurement as an index of torque during dynamic exercise. *Physiol.* **35** (Suppl.), 115–116.

BLIGHT, A. R. (1976). Undulatory swimming with and without waves of contraction. *Nature* **264**, 352–354.

BLIGHT, A. R. (1977). The muscular control of vertebrate swimming movements. *Biol. Rev.* **52**, 181–218.

CRENSHAW, H. C. (1992). A technique for tracking spermatozoa in three dimensions without viscous wall effects. *Proc. VI Int. Congress Spermatology*. Siena, Italy: Raven Press.

CURTIN, N. A. AND WILLIAMS, T. L. (1990). Force during shortening and stretch of active muscle fibers isolated from the lamprey, *Ichthyomyzon unicuspis*. *J. Physiol., Lond.* **430**, 67P.

DANIEL, T. L. (1984). Unsteady aspects of aquatic locomotion. *Am. Zool.* **24**, 121–134.

DEN HARTOG, J. P. (1956). *Mechanical Vibrations.* 4th edn. New York: McGraw-Hill.

DENNY, M. W. (1988). *Biology and the Mechanics of the Wave-Swept Environment.* Princeton, NJ: Princeton University Press.

GILLET, P. (1984). *Calculus and Analytical Geometry*. 2nd edn. Lexington, MA: D. C. Heath.

HESS, F. AND VIDELER, J. J. (1984). Fast continuous swimming of saithe (*Pollachius virens*): a dynamic analysis of bending moments and muscle power. *J. exp. Biol.* **109**, 229–251.

HOME, E. (1809). On the nature of the intervertebral substance in fish and quadrupeds. *Proc. R. Soc. Lond.* **16**, 177–187.

JAYNE, B. C. AND LAUDER, G. V. (1993). Red and white muscle activity and kinematics of the escape response of the bluegill sunfish during swimming. *J. comp. Physiol.* A **173**, 495–508.

LONG, J. H., JR (1992). Stiffness and damping forces in the intervertebral joints of blue marlin (*Makaira nigricans*). *J. exp. Biol.* **162**, 131–155.

LONG, J. H., JR (1994). Morphology, mechanics and locomotion: the relation between the notochord and swimming speed in sturgeon. *Env. Biol. Fishes* (in press).

ROCKWELL, H., EVANS, F. G. AND PHEASANT, H. C. (1938). The comparative morphology of the vertebrate spinal column: its form as related to function. *J. Morph.* **63**, 87–117.

ROME, L. C., CHOI, I.-H., LUTZ, G. AND SOSNICKI, A. (1992). The influence of temperature on muscle function in the fast swimming scup. I. Shortening velocity and muscle recruitment during swimming. *J. exp. Biol*. **163**, 259–279.

ROME, L. C., SWANK, D. AND CORDA, D. (1993). How fish power swimming. *Science* **261**, 340–343.

SEJERSTED, O. M., HARGENS, A. R., KARDEL, K. R., BLOM, P., JENSEN, O. AND HERMANSEN, L. (1984). Intramuscular fluid pressure during isometric contraction of human skeletal muscle. *J. appl. Physiol.* **56**, 287–295.

SIMMS, E. L. AND BURDICK, D. S. (1988). Profile analysis of variance as a tool for analyzing correlated responses in experimental ecology. *Biometr. J.* **2**, 229–242.

SYMMONS, S. (1979). Notochordal and elastic components of the axial skeleton of fishes and their functions in locomotion. *J. Zool., Lond.* **189**, 157–206.

VAN LEEUWEN, J. L., LANKHEET, M. J. M., AKSTER, H. A. AND OSSE, J. W. M. (1990). Function of red axial muscles of carp (*Cyprinus carpio*): recruitment and normalized power output during swimming in different modes. *J. Zool., Lond*. **220**, 123–145.

VOGEL, S. (1981). *Life in Moving Fluids*. Princeton, NJ: Princeton University Press (1983 reprint).

WAINWRIGHT, S. A. (1983). To bend a fish. In *Fish Biomechanics* (ed. P. Webb and D. Weihs), pp. 68–91. New York: Praeger.

WAINWRIGHT, S. A., VOSBURGH, F. AND HEBRANK, J. H. (1978). Shark skin: function in locomotion. *Science* **202**, 747–749.

WASSERSUG, R. J. (1989). Locomotion in amphibian larvae (or 'why aren't tadpoles built like fishes?') *Am. Zool.* **29**, 65–84.

WASSERSUG, R. J. AND VON SECKENDORFF HOFF, K. (1985). The kinematics of swimming in anuran larvae. *J. exp. Biol.* **119**, 1–30.

WEBB, P. W. (1986). Kinematics of lake sturgeon, *Acipenser fulvescens*, at cruising speeds. *Can. J. Zool.* **64**, 2137–2141.

WEBB, P. W. (1988). 'Steady' swimming kinematics of tiger musky, an esociform accelerator and rainbow trout, a generalist cruiser. *J. exp. Biol.* **138**, 51–69.

WEBB, P. W. AND KEYES, R. S. (1982). Swimming kinematics of sharks. *Fishery Bull. Fish. Wildl. Serv. U.S.* **80**, 803–812.
WEIHS, D. (1989). Design features and mechanics of axial locomotion in fish. *Am. Zool.* **29**, 151–160.
WESTNEAT, M. W., HOESE, W., PELL, C. A. AND WAINWRIGHT, S. A. (1993). The horizontal septum: mechanisms of force transfer in locomotion of scombrid fishes (Scombridae, Perciformes). *J. Morph.* **217**, 183–204.
WILKINSON, L. (1989). *SYSTAT: The System for Statistics*. Evanston, IL: SYSTAT, Inc.
WILLIAMS, T. L., GRILLNER, S., SMOLJANINOV, V. V., WALLEN, P., KASHIN, S. AND ROSSIGNOL, S. (1989). Locomotion in lamprey and trout: the relative timing of activation and movement. *J. exp. Biol.* **143**, 559–566.
WITHERS, P. C. (1992). *Comparative Animal Physiology*. New York: Saunders College Publishing.